CONTINENTAL RAYLEIGH WAVE DISPERSION AND THE ESTIMATION OF CHIRPFILTER DETECTORS

William Tucker, et al

Southern Methodist University

Prepared for:

Air Force Office of Scientific Research

March 1973

TECHNICAL REPORT

to the

AIR FORCE OFFICE OF SCIENTIFIC RESEARCH

from

William Tucker

John A. McDonald

and

Eugene Herrin

Dallas Geophysical Laboratory
Southern Methodist University
Dallas Texas 75275

ARPA Order No: 1827-1
Program Code: 2F10
Name of Contractor: Southern Methodist University
Effective Date of Grant: 1 July 1971
Grant Expiration Date: 30 June 1973
Amount of Grant Dollars: $179,739
Grant Number: 71-2133B
Principal Investigator: Eugene Herrin
AC 214/692-2760
Program Manager: Truman Cook
AC 214/692-2031
Title of Work: Identification of Earthquakes and Underground Explosions
University Account Number: 80-46

Sponsored by
Advanced Research Projects Agency

Approved for public release;
distribution unlimited.

CONTINENTAL RAYLEIGH WAVE DISPERSION AND THE ESTIMATION OF CHIRP-FILTER DETECTORS

William Tucker
John A. McDonald
Eugene Herrin

March 1973

Dallas Geophysical Laboratory
Southern Methodist University
Dallas Texas 75275

ABSTRACT

Rayleigh wave data were recorded by a single vertical high-gain seismograph located in north Texas. It was found that Rayleigh waves propagating in a continental path over the pole to this station exhibited very stable dispersion characteristics, particularly in the period range 35-75 secs: at shorter periods an average dispersion curve could be estimated. A composite dispersion curve was used to develop "chirp" (or matched) filters, the form of which depended on the distance between the seismograph and the event. Such filters are shown to be very efficient in improving the signal-to-noise ratio of Rayleigh waves emanating from events in the Sino-Soviet region and can be used as a means of separating "mixed" Rayleigh waves. For the path over the pole (or "polar waveguide") the detection threshold is estimated to be at $M_s = 3.5$.

UNCLASSIFIED
Security Classification

DOCUMENT CONTROL DATA - R & D

(Security classification of title, body of abstract and indexing annotation must be entered when the overall report is classified)

1. ORIGINATING ACTIVITY (Corporate author)
Southern Methodist University
Dallas Geophysical Laboratory
Dallas, TX 75275

2a. REPORT SECURITY CLASSIFICATION
UNCLASSIFIED

2b.

3. REPORT TITLE
CONTINENTAL RAYLEIGH WAVE DISPERSION AND THE ESTIMATION OF CHIRPFILTER DETECTORS

4. DESCRIPTIVE NOTES (Type of report and inclusive dates)
Scientific.....Interim

5. AUTHOR(S) (First name, middle initial, last name)
William Tucker, John A. McDonald, and Eugene Herrin

6. REPORT DATE	7a. TOTAL NO. OF PAGES	7b. NO. OF REFS
March 1973	46 46	18

8a. CONTRACT OR GRANT NO.	9a. ORIGINATOR'S REPORT NUMBER(S)
AFOSR-71-2133	
b. PROJECT NO. AO 1827	
c. 6270 D	9b. OTHER REPORT NO(S) (Any other numbers that may be assigned this report) AFOSR - TR - 73 - 1010
d.	

10. DISTRIBUTION STATEMENT
Approved for public release;
distribution unlimited.

11. SUPPLEMENTARY NOTES	12. SPONSORING MILITARY ACTIVITY
TECH, OTHER	AF Office of Scientific Research/NP 1400 Wilson Boulevard Arlington, VA 22209

13. ABSTRACT

Rayleigh wave data were recorded by a single vertical high-gain seismograph located in north Texas. It was found that Rayleigh waves propagating in a continental path over the pole to this station exhibited very stable dispersion characteristics, particularly in the period range 35-75 secs: at shorter periods an average dispersion curve could be estimated. A composite dispersion curve was used to develop "chirp" (or matched) filters, the form of which depended on the distance between the seismograph and the event. Such filters are shown to be very efficient in improving the signal-to-noise ratio of Rayleigh waves emanating from events in the Sino-Soviet region and can be used as a means of separating "mixed" Rayleigh waves. For the path over the pole (or "polar waveguide") the detection threshold is estimated to be at M_s=3.5.

DD FORM 1 NOV 65 1473

UNCLASSIFIED
Security Classification

INTRODUCTION

Ewing and Press (1952) described the classical "peak-and-trough" method of determining a fundamental dispersion curve from a single surface wave coda. Satô (1955) applied Fourier analysis to the calculation of dispersion curves. These techniques have been improved upon (Block and Hales, (1968), Landisman, et al (1969) and Dziewonski, et al (1969)), and an overall processing system was devised combining Fourier analysis and time-varying filters, enabling the calculation of, not only the fundamental phase and group velocity curves, but also the curves for the higher modes. In particular, once a group velocity curve has been obtained it is possible to design a time varying filter that extracts a single dispersed mode and effects a significant improvement in the signal-to-noise ratio. The filtered output is then an estimate of the true signal. Dziewonski, et al (1968) summarizes these methods and it is evident that they extract the maximum amount of information from the surface wave signal. Nevertheless, the methods are both time consuming and computationally difficult. But if we restrict the investigation to the fundamental mode of surface wave propagation, it becomes

possible to develop a fast, simple digital technique for the analysis.

In this paper we describe a scheme which estimates the fundamental group velocity dispersion curve from a seismogram, and then constructs a "matched" filter based on the estimated curve. This matched, or chirp, filter can then be used to operate on signals with low signal-to-noise ratios.

THE SEISMOGRAMS

During the period March through August 1970 a three-component seismograph system was operated at a depth of 180 m in the Morton Salt Company mine at Grand Saline, Texas (Sorrells et al., 1971). The seismometers were sealed in such a manner that the masses were not subject to buoyancy effects from atmospheric pressure changes. The systems were of the "advanced" long period type which are operated with a peak magnification at a period of 50 secs. Sorrells et al. (1971) have shown that if such a system is operated at a site which is remote from seismic noise generated by atmospheric processes, the spectra of the long period noise exhibits a minimum in the period range 20-60 sec. Careful installation of these seismographs at a depth of about 180 m enabled the vertical seismograph, the only one used in the present study, to be operated at a magnification of 200,000. The data were recorded on a digital acquisition system described by Herrin and McDonald (1971) after sampling at a rate of 1 per second.

The recorded seismograms were associated with source parameters and body wave magnitudes provided in Preliminary Determination of Epicenters (PDE) issued by NOAA.

DISPERSION CURVE ESTIMATION

A computer program was written which enabled analog representations of digital time series to be displayed on an oscilloscope. Selected seismograms were then plotted, using a Cal-comp plotter. It was decided to limit the observations to Rayleigh waves recorded at teleseismic distance which had traversed a predominantly continental path; thus restricting the range of azimuths to about 15^{o} east and west of the pole, and the range of epicentral distances to 55^{o}-130^{o}.

Using the plot of the seimogram an estimation was made of the start time (T_s) and the length, in seconds, (window) of the Rayleigh signal. A computer program was written which searched this window, starting at T_s, for zero crossings, in a manner similar to the "peak and trough" technique of Ewing and Press, (1952). The time of the "actual" zero crossing was calculated by triangulation between the last point immediately prior to a zero crossing, and the first point immediately after it. The initial zero crossing time, (T_0) was stored, and at the next zero crossing, (T_1) the first period, (P_1) was computed. T_1 and P_1 were then stored and the seach continued until the window was exhausted. For i = 1, 2, ..., N, the group velocites and the periods were computed from

$$V_i = \frac{\Delta}{TT_i} \quad \text{and} \quad P_i = 2\,(T_i - T_{i-1}),$$

where N = the number of zero crossings in the window,

Δ = the epicentral distance from event to station in km, and

TT_i = the observed travel time from source to the ith zero crossing.

Since the actual zero crossing occurred within a one second interval any variation must be less than one second. As a conservative approximation, we assumed the error to be uniform; thus the variance was 1/12 sec^2.

Now $TT_i = T_i - 0$

where 0 is the origin time of the event. From Herrin et al. (1968) a reasonable origin time variance is 0.81 to 1.00 sec^2. Since T_i and 0 are independent observations their variances may be added. We thus take 1.00 sec^2 as a reasonable variance for each TT_i. From Tucker et al. (1968) and Herrin et al. (1968) a reasonable variance in Δ is 900 km^2. We then have

$$V_i = \frac{\Delta + e_1}{TT_i + e_2},$$

where Δ = the true distance (in km)

TT_i = the true travel time,

e_1 = the error in epicentral distance (σ_1=30 km),

e_2 = the error in travel time (σ_2= 1 sec).

Assuming an event with Δ = 6000 km and a maximum group velocity of 4.00 km/sec (Oliver, 1962) then

$$V_1 = (6000 + e_1)/(1500 + e_2).$$

Since the variance of e_2 is small relative to 1500 we can ignore e_2 and write

$$V_1 = 4.0 + e_1/1500$$
$$= 4.0 + \delta_1,$$

where

$$\sigma^2_{\delta_1} = 0.0004 \text{ sec}^2.$$

For a lower period cutoff of 20 sec (or a velocity of 3.00 km/sec) we get

$$V_N = (6000 + e_N)/2000$$
$$= 3.0 + e_N/2000$$
$$= 3.0 + \delta_2,$$

where

$$\sigma^2_{\delta_2} = 0.000225 \text{ sec}^2.$$

Thus as a conservative approximation we can assume

$$V_i = \text{True velocity } i + \delta$$

where $\sigma_\delta^2 = 0.0004 \text{ sec}^2$.

Let us now consider the variation in the P_i.

We have

$$P_i = 2(T_i - T_{i-1})$$

where

$$\sigma_{T_i}^2 = 0.0833 \text{ sec}^2.$$

Since the minimum period is assumed to be 20 sec the minimum time difference is of the order of 10 sec and we may assume that the errors in T_i and T_{i-1} are independent. Then the variance of a P_i is

$$\sigma_{P_i}^2 = 4(0.0833 + 0.0833) = 0.6664 \text{ sec}^2.$$

Thus the variance in a velocity observation is three orders of magnitude less than that of a period observation. We therefore ignored the error in the velocity computations and assumed that the velocities were known without error. Now assuming that all the error lies in the period computations, it is possible to consider a group velocity curve as a regression of period on group velocity.

Figure 2 shows the data points obtained from dispersed

Rayleigh waves for three events located in the Arctic (Table 1) at similar epicentral distances and similar azimuths. Data from an event in Sinkiang Province along a similar azimuth, but at a greater distance, (Table 1) are shown in Figure 3. A comparison of the data in Figures 2 and 3 in the velocity range 3.50 to 3.90 km/sec (periods approximately 35 and 75 sec respectively) indicates that there is no statistical difference between the true dispersion curve for each event. The observed scatter could result from statistical fluctuations in the estimates or real differences in the velocity-period relationship along the propagation path. Thus it appears that in the velocity range 3.50 to 3.90 km/sec there is a unique dispersion curve independent of path.

However, in the velocity range 2.90 - 3.5 km/sec (periods of 20-35 sec), there are indications that real differences may exist between the true dispersion curves in Figures 2 and 3. In this velocity range we estimated, for the purposes of this study, an average dispersion curve.

Using group velocity as the independent variable the data for each event were grouped into cells of width 0.5 km/sec. Within each cell the data were ordered according to period value and the sample median was computed. The cell midpoint

velocities and median periods were stored as data pairs. The sample median was chosen as a measure of central tendency because it is more efficient than the sample mean in the presence of outliers (Dixon, 1953)

In the velocity range 3.50 to 4.00 km/sec the sample median periods are observations on a single curve; therefore, adjacent points are related and a smoothing operator should improve the results. Furthermore, in the velocity range 2.90 to 3.50 km/sec only a representative smooth curve was desired, and a three point moving average operator was applied to the sample period values. The operator is given by

$$\text{Period (1)} = X(1)$$

$$\text{Period (Num)} = 1/2 \cdot X(\text{Num}-1) + 1/2 \cdot X(\text{Num})$$

$$\text{Period (i)} = 1/4 \cdot X(i-1) + 1/2 \cdot X(i) + 1/4 \cdot X(i+1)$$

where $1 = 2, \ldots, \text{Num}-1$

1 = the index of the cell with the largest velocity

Num = the index of the cell with the smallest velocity

X(i) = the sample median period of cell i

Period (i) = the smoothed period of cell i.

The resulting dispersion curves for the four events (Figures 2 and 3) are shown in Figure 4. The smoothed curves show the same results as the original zero crossing data. That is, the curves are not statistically different in the velocity range 3.50 to 3.90 km/sec, and, in the range 2.90 to 3.50 km/sec, the smoothed curves indicate that the actual paths do not produce markedly different dispersions curves at these short periods.

In view of the similarity of the curves we combined the data from the four events and estimated a composite group velocity dispersion curve shown in Figure 5. Also shown in this figure is the continental dispersion curve compiled by Oliver (1962); the long dashed lines indicate bounds of the expected scatter under normal observational conditions. The composite curve can be seen to fall within the error bounds. Furthermore, the composite curve is in good agreement with the results of Ewing and Press (1956) who reported a group velocity of about 3.9 km/sec at a period of 75 sec. The smoothed data points are given in tabular form in Table 2.

CHIRP FILTER CONSTRUCTION

We have shown that, for our seismograph station in north Texas, we can assume a single group velocity dispersion curve for the continental path over the pole. We can then design "matched", or chirp, filters to aid in the detection of surface waves from small earthquakes traversing the same path.

A program was written which produced a sine wave that decreased in period with time, the dispersion being a function of epicentral distance. Such waveforms have been given the name "chirp" in radar technology. In this case the information used to distance - function were from Table 2. The following assumptions were made:

(i) the first arriving energy is at the maximum period observed, and

(ii) between the data points of Table 2 the dispersion curve is linear.

With these assumptions we obtained, by simple algebraic manipulations,

$$TT_i = \Delta / V_i \quad \text{and} \quad T_o = TT_i - P_{1/2},$$

and for the ith linear segment

$$w_i(t) = \frac{2\pi (t+T_o)(1/TT_{i-1} - 1/TT_i)}{\left[P_{i-1} - P_i - (P_{i-1}/TT_i - P_i/TT_{i-1})(t+T_o)\right]},$$

where $$(T_{i-1} - T_o) \leq t \leq (T_i - T_o),$$

$w_i(t)$ = frequency in radians for the t th time,

P_i = the i th period in sec,

TT_i = the i th travel time in sec,

i = 1, 2, ..., Num.

The dispersed sine wave computations were given by

$$AMP(k) = \sin\left[w_i(t).k + \rho_i\right],$$

where $k = 1, 2, \ldots, N_i$

N_i = the number of data points in the i th segment

ρ_i = phase shift of the i th segment

AMP(k) = the dispersed sine wave amplitude.

For k = 1 the segment was extrapolated to include time points back to T_0. For all other values of k only time points between the TT_i were included in a given segment.

The ρ_i were as follows

$$\rho_1 = 0$$

$$\rho_i = w_i(t_{max}) + \rho_{i-1},$$

for 1 = 2, 3, ..., Num, where t_{max} is the largest t value in the i th segment. Also

$$t = k + TT_{i-1}$$

so that

$$t_{max} = N_i + TT_{i-1}.$$

In each linear segment the frequency was a function of time given by $w_i(t)$. The origin of the sine wave was taken as zero, which gave the time shift between t and k. The phase shift ρ_i ensured a smooth transition from segment to segment.

In Figure 6 we show the dispersed sine wave for one of the events used in calculating the composite dispersion curve (Figure 5). These sinusoids indicate the effects of differences in epicentral distance; for the Sinkiang Province event ($\Delta = 107.6^{\circ}$) the first zero crossing occurs at about 72 sec and for the other three (Δ = approximately 60°) the first zero crossing occurs at about 68 sec. Similar period differences are evident throughout the curves.

Convolution of these dispersed sine waves, or chirp filters, with their respective signals should then produce

psuedo-autocorrelation functions. The results are not true autocorrelations because the sine waves have not been amplitude modulated; nor is the "true" dispersion given exactly by the composite dispersion curve.

APPLICATION OF THE CHIRP FILTER

The chirp filter constructed from the dispersion curve in Figure 5 was applied to four different sets of seismograms. First, it was convolved with the original seismograms used to construct the dispersion curve; second, with other events remote from the first four; third, as detector of surface waves with a low signal-to-noise ratio; and fourth, as a means of separating "mixed" Rayleigh waves.

In order to remove very long period energy each seismogram was filtered prior to being convolved with the chirp filter. The high-pass digital filter used had a corner at 50 sec and fell at 36 db/octave to a minimum at a period of 100 sec.

Figure 7 shows the application of the chirp filter to the time series for each of the events used in calculating the composite dispersion curve. In each example the lower trace shows the filter output, correctly aligned with the input time series. The auto-correlation-like nature of the output should be noted; the maximum peak of which should occur at the beginning of the Rayleigh wave energy. In each of the figures the data were plotted so that the largest excursion was full-scale; therefore, the improvement in signal-to-noise ratio

can be estimated by examining the reduction in noise.

Three other events were selected (table 3) with similar continental polar surface wave paths to Texas; however, their epicenters were remote from those given in table 1. The results of convolving these seismograms with the same chirp filter used previously are shown in figure 8. The outputs clearly show that the filter is effective for widely separated sources.

Figure 9 shows the results of convolving the chirp filter with seismograms in which the surface waves are barely discernible. This figure shows a seismogram from a small event ($m_b = 4.7$) at a depth of 110 km in the Hindu-Kush; convolution clearly emphasized the start of the surface waves.

Mixed Rayleigh waves resulting either from multiple sources close together or from reflections, or from multi-pathing are very difficult to separate, even when data from large arrays are avialable. However, if the arrivals are separated by times greater than about 50 sec, the chirp filter technique can be useful in separating the arrivals. Figure 10(a) (lower trace) shows the filtered output for a small event from the region of the USSR-Mongolia border;

two and, possibly, three Rayleigh wave arrivals can be seen on the filtered trace. The first and largest of these arrivals occurs precisely at the expected arrival time of the fundamental Rayleigh wave for this event. A fairly large earthquake (m_b = 5.9) sparked an earthquake swarm from this region of the USSR-Mongolia border in May 1970. Another earthquake from the swarm is shown in figure 10(b); again convolution detected two arrivals. All available seismograms of earthquakes in the swarm were processed but only three showed multiple detections of surface waves.

DISCUSSION

We have described above a new approach to the "peak and trough" method of surface wave analysis which has been used to determine group velocity dispersion curves. The machine measurements proved to be at least as good as those of an experienced analyst, and could be produced much faster.

A further advantage was gained in the present analysis from the special properties of the seismograph system. Many previous surface wave studies have used data from the World-Wide Standard Seismograph Network recordings in which the peak period of the calibration response is at 20 sec. In our systems, the peak response proved to lie within the "stable"portion of the group velocity dispersion curve.

This type of analysis, while being quick and computationally easy, nevertheless has its problems. Any non-least-time arrivals will impair the estimation of the dispersion curve; the technique does not give as much information as that of Dziewonski et al. (1969), which places a restriction on the use of the method.

Nevertheless, by carefully selecting events with a large signal-to-noise ratio, and with an absence of either higher modes or very long period surface waves, it has been

shown that a single fundamental group velocity dispersion curve can be calculated for a continental path over the pole to the central United States. This claim can be further substantiated by the fact that a chirp filter, constructed from this fundamental dispersion curve, proved effective for events from a region extending from southern USSR and northern China to the Arctic Ocean.

In addition to the events mentioned in the previous sections of this paper, seismograms from the other events listed in table 3 were prccessed. In some cases the auto-correlations displayed low signal-to-noise ratios, but in every search for an event reported by NOAA, an event was detected; unreported events were also detected. Thus further study is required to determine operational detection thres-holds and false alarm rates.

CONCLUSIONS

In view of the results reported here it might be appropriate to suggest a reason for the stability of the group velocity dispersion curve, particularly at the longer periods, on a continental path over the pole.

It has been shown in recent years (e.g. Roy et al. 1972) that the western United States, known structurally as the Basin and Range Province, is characterized by high temperatures in the lower crust and upper mantle. This region, which is known to extend up the western part of Canada, is also a poor transmitter of long period surface waves. A particularly good example of this phenomenum can be seen in figure 11. The Greenland Sea event (table 1), as recorded at Grand Saline, is compared to the same event recorded at Queen Creek, Arizona. This station (Fix and Sherwin, 1970) is located in the heart of the Basin and Range Province. The gains of the seismographs at the two stations were equalized at 50 sec, but it will be seen that the longer period surface waves are virtually missing at the Queen Creek site.

To the east the continental United States are characterized by the Atlantic and Gulf coastal plains. Furthermore, the central plains are known to have relatively low temperatures

in the lower crust and upper mantle (Roy, et al., 1968, Combs and Simmons, 1973) which provides an exceptionally good path for Rayleigh waves with periods from 20-75 sec. Our detection station in north Texas is, essentially, at the southern end of a surface wave guide which passes over the north pole (Figure 12).

The analog plots of the seismograms used in the study were analysed, after they had been high-pass filtered, for the presence of detectable Rayleigh waves. Using the formula

$$M_s = \log \frac{(A)}{(T)} + 1.66 \log \Delta - 0.18, \text{ which}$$

can be easily derived (Gutenberg, 1945), values of M_s were found where A is the peak-to-peak amplitude, in mμ, of the surface wave at a period of T=20 sec, and Δ is the distance from epicenter to detector, in degrees. The results of these computations are given in tables 1 and 3, where the values of M_s are compared to the values of m_b determined by NOAA.

Using the data presented in this study an interim detection threshold has been determined for our Grand Saline recording station. For events travelling within the polar waveguide this threshold is at $M_s = 3.5$, for a single vertical seismometer, which is equivalent to a threshold of $m_b = 4.5$ for events at depths of less than 50 km.

ACKNOWLEDGEMENTS

Nancy Cunningham was responsible for much of the software developments used in this research, Frank P. Van Leer was responsible for the initial seismic analysis. The research was supported by the Air Force Office of Scientific Research under Grant No. 71-2133B.

REFERENCES

Bloch, S. and A. L. Hales (1969). New techniques for the determination of surface wave phase velocities, Bull. Seism. Soc. Am. 58, 1021-1034.

Combs, J. and G. Simmons, Terrestial heat flow determinations in north central United States, J. Geophys. Res., 78, 441-461, 1973.

Dixon, W. J. (1953). Processing data for outliers, Biometrics 9, 74-89.

Dziewonski, A., M. Landisman, S. Bloch, Y. Sato and S. Asano (1968). Progress report on recent improvements in the analysis of surface wave observations, Journal of Physics of the Earth, Special Issue 16, 1-26.

Dziewonski, A., S. Bloch and M. Landisman (1969). A technique for the analysis of transient seismic signals, Bull. Seism. Soc. Am. 59, 427-444.

Ewing, Maurice and Frank Press (1952). Crustal structure and surface wave dispersion, pt. 2, Bull. Seism. Soc. Am. 42, 315-325.

Ewing, Maurice and Frank Press (1956). Rayleigh wave dispersion in the period range 10 to 500 seconds, Trans. Am. Geophys. Union 37, 213-215.

Fix, J. E. and J. R. Sherwin, A high-sensitivity strain/inertial seismograph installation, Bull. Seis. Soc. Am., 60, 180-3-1822, 1970.

Gutenberg, B., Amplitudes of surface waves and magnitudes of shallow earthquakes, Bull. Seis. Soc. Am., 35, 3-12, 1945.

Herrin, Eugene, William Tucker, James Taggart, David W. Gordon and John L. Lobdell (1968). Estimation of surface focus P travel times, Bull. Seism. Soc. Am. 58, 1273-1291.

Herrin, Eugene and John A. McDonald (1971). A digital system for the acquisition and processing of geoacoustic data, Geophys. J. R. Astr. Soc. 26, 13-20.

Landisman, M. A., A. Dqiewonski and Y. Sato (1969). Recent improvements in the Analysis of surface wave observations, Geophys. J. R. Astr. Soc. 17, 369-403.

Oliver, Jack (1962). A summary of observed seismic surface wave dispersion, Bull. Seism. Soc. Am. 52, 81-86.

Roy, R. F., E. R. Decker, D. D. Blackwell and F. Birch, Heat flow in the United States. J. Geophys. Res., 73, 5207-5221, 1968.

Roy, R. F., D. D. Blackwell and E. R. Decker (1972). Continental heat flow, in Nature of the Solid Earth, ed. E. C. Robertson, McGraw-Hill, New York, 506-543.

Sato, Y. (1955). Analysis of dispersed surface waves by means of Fourier Transform 1, Bull. Earthquake Res. Inst., Tokyo Univ., Part 1, 33, 33-47.

Sorrells, G. G., John A. McDonald, Z. A. Der and Eugene Herrin (1971). Earth motion caused by local atmospheric pressure changes, Geophys. J. R. Astr. Soc. 26, 83-98.

Tucker, William, Eugene Herrin and Helen W. Freedman (1968). Some statistical aspects of the estimation of seismic travel times, Bull. Seism. Soc. Am. 58, 1243-1260.

FIGURE CAPTIONS

1. Response of the seismograph system.

2. Rayleigh wave dispersion information recorded in north Texas for three events (see table 1), (a) North of Svalbard, (b) Greenland Sea, (c) Norwegian Sea.

3. Rayleigh wave dispersion information recorded in north Texas for an event in Sinkiang Province (see table 1).

4. Rayleigh wave dispersion curves for the four events in table 1 after smoothing (a) North of Svalbard (b) Greenland Sea (c) Norwegian Sea (d) Sinkiang Province.

5. Composite Rayleigh wave dispersion curve for the four events in table 1 in conjunction with continental dispersion curve due to Oliver (1962).

6. Typical dispersed sine wave, or chirp filter, derived from the dispersion curve shown in figure 4 (b).

7. Convolution of the chirp filter derived from the curve in figure 5 with each of the four events given in table 1, (a) North of Svalbard, (b) Greenland Sea (c) Norwegian Sea (d) Sinkiang Province.

8. Convolution of the chirp filter derived from the curve in figure 5 with three of the events given in table 3: events from very different locations.

9. Convolution of the chirp filter derived from the curve in figure 5 with an event from the Hindu-Kush (table 3) in which surface waves are barely discernible.

10. Convolution of filter and surface waves showing two, or possibly, three surface wave arrivals (a) USSR Mongolian border on 17 May 1970, m_b = 4.5, (b) USSR - Mongolian border on 23 May 1970, m_b = 4.5. (See table 3 for details).

11. Comparison of the surface waves from the Greenland Sea event (table 1) recorded at (a) Queen Creek, Arizona, (b) Grand Saline, Texas.

12. A polar plot of the world centered on Grand Saline. The locations of the epicenters of the events used in this study are shown; the alphanumeric designation refers to tables 1 and 3.

TABLE CAPTIONS

1. Data for the four events used to calculate the composite dispersion curve shown in figure 5.
2. Coordinates of the points used to plot the curve in figure 5.
3. Data for the other events used in this study.

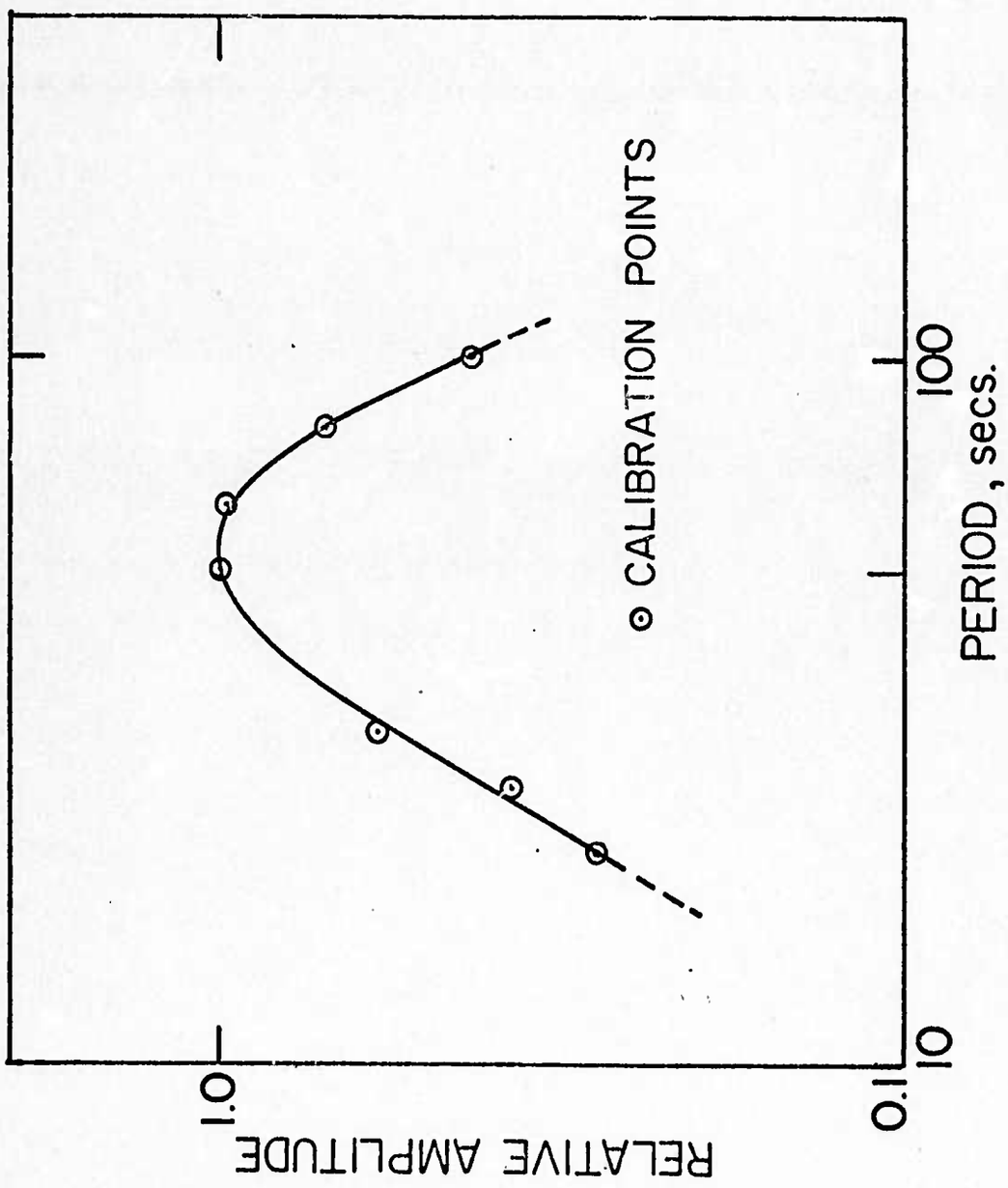
RELATIVE AMPLITUDE
1.0
0.1
10
100
PERIOD, secs.
⊙ CALIBRATION POINTS

Figure 1

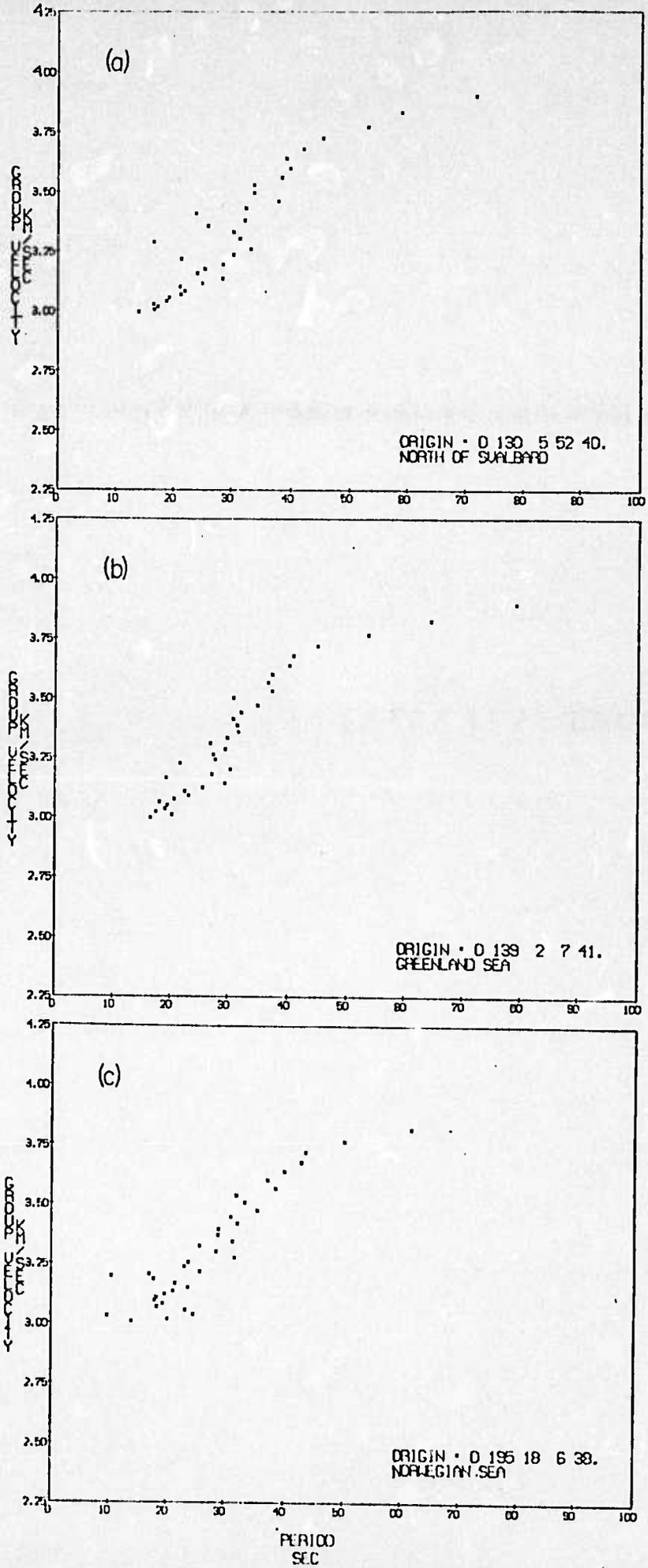
(a)
ORIGIN • D 130 5 52 40.
NORTH OF SVALBARD
(b)
ORIGIN • D 139 2 7 41.
GREENLAND SEA
(c)
ORIGIN • D 195 18 6 38.
NORWEGIAN SEA
GROUP VELOCITY KM/SEC
PERIOD SEC

Figure 2

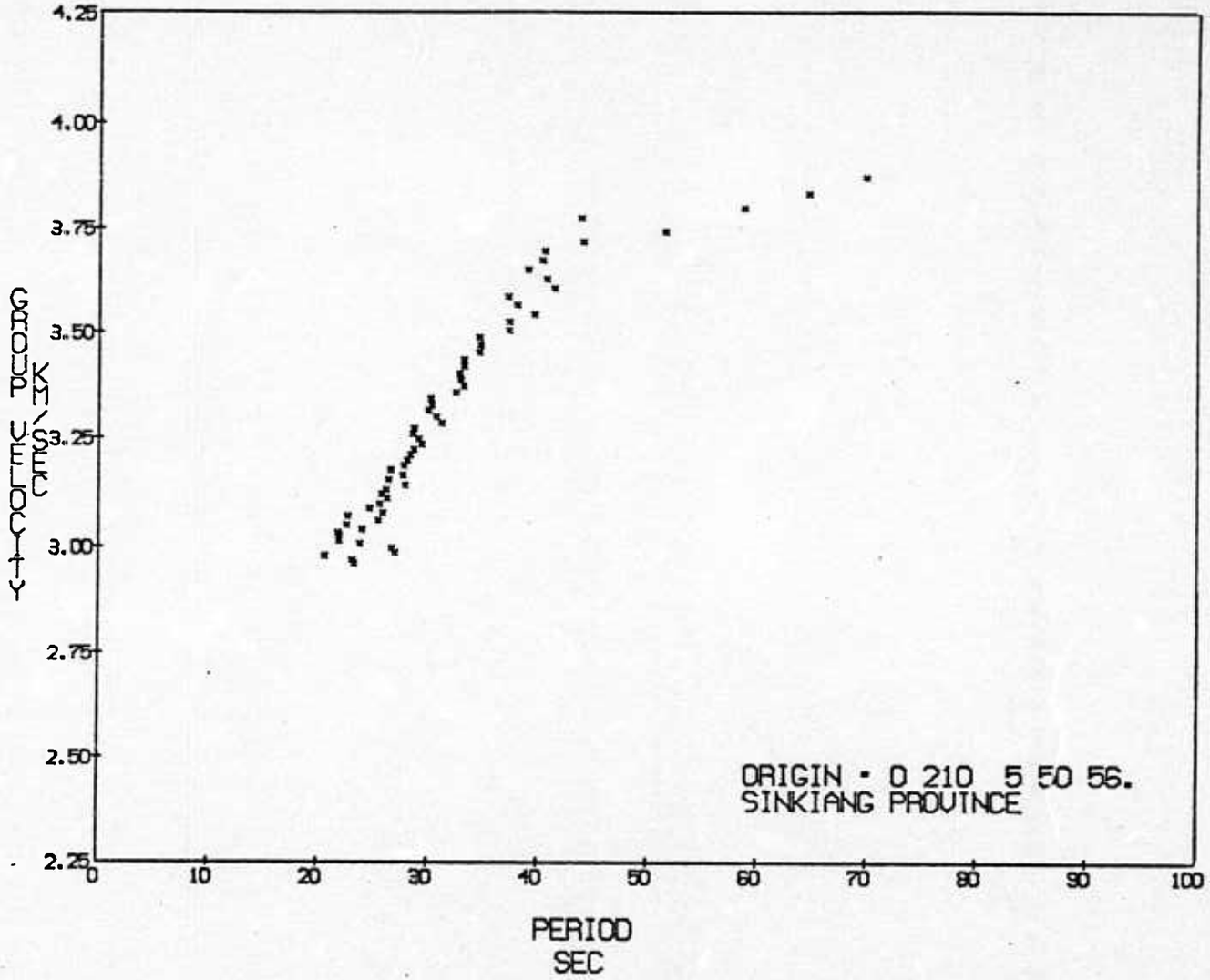
4.25
4.00
3.75
3.50
3.25
3.00
2.75
2.50
2.25
GROUP VELOCITY KM/SEC
0
10
20
30
40
50
60
70
80
90
100
PERIOD
SEC
ORIGIN - 0 210 5 50 56.
SINKIANG PROVINCE

Figure 3

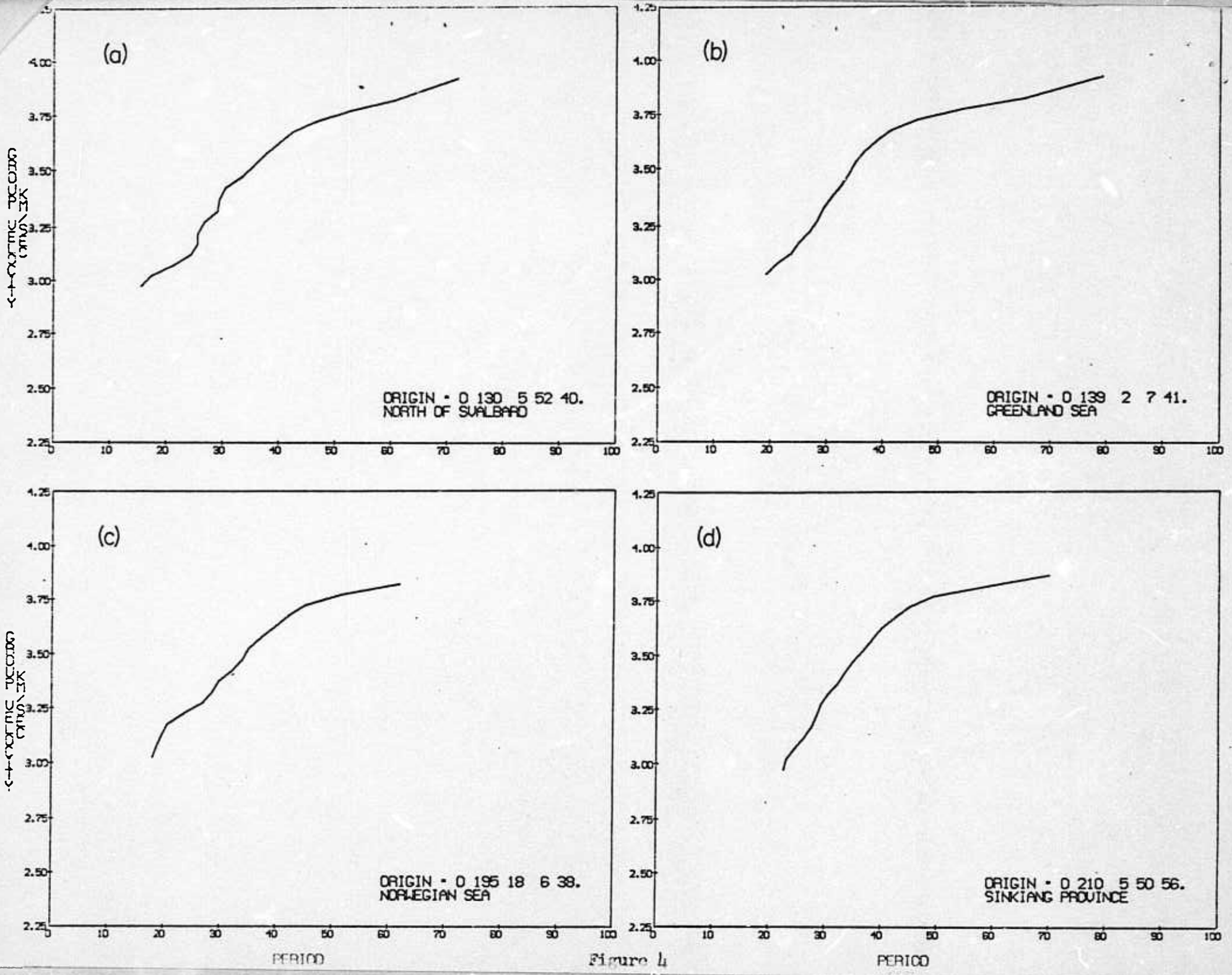
(a)
ORIGIN - 0 130 5 52 40.
NORTH OF SVALBARD
(b)
ORIGIN - 0 139 2 7 41.
GREENLAND SEA
(c)
ORIGIN - 0 195 18 6 38.
NORWEGIAN SEA
(d)
ORIGIN - 0 210 5 50 56.
SINKIANG PROVINCE
PERIOD
PERIOD

Figure 4

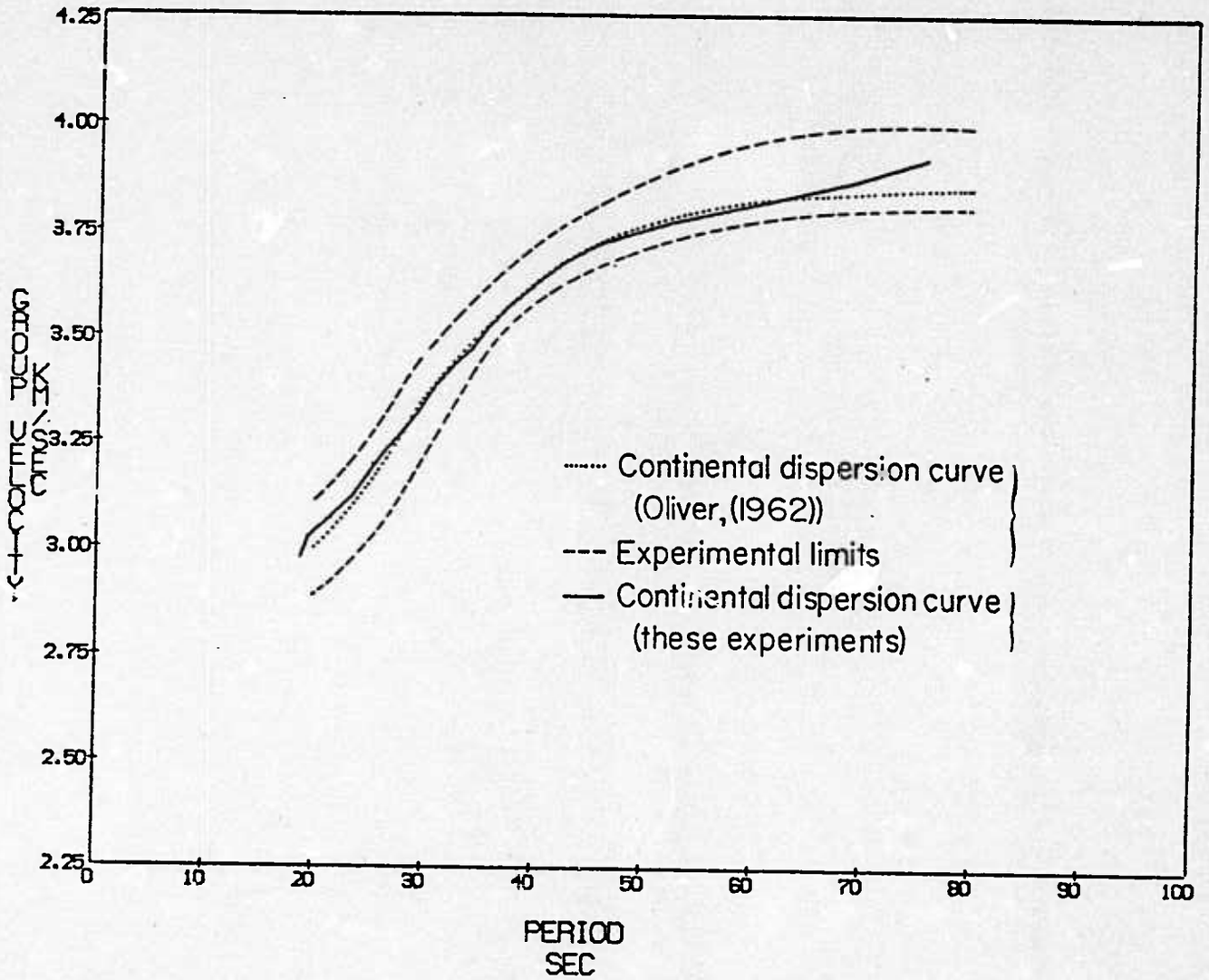
1.25
4.00
3.75
3.50
3.25
3.00
2.75
2.50
2.25
0
10
20
30
40
50
60
70
80
90
100
PERIOD
SEC
Continental dispersion curve
(Oliver, (1962))
Experimental limits
Continental dispersion curve
(these experiments)

Figure 5

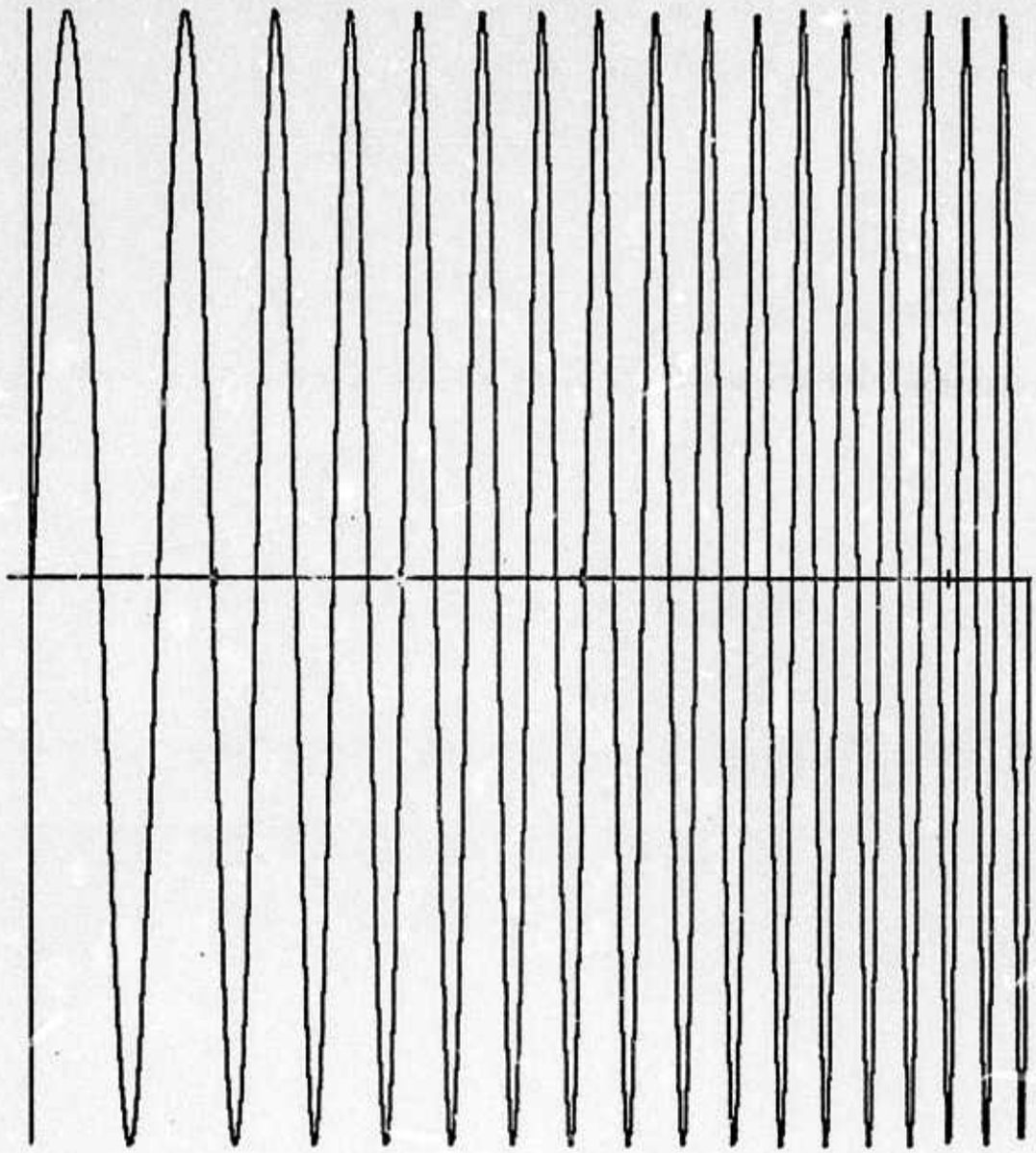

DISPERSED SINE WAVE
GREENLAND SEA
DELTA = 59.70
TICK MARKS EVERY 100 SEC

Figure 6

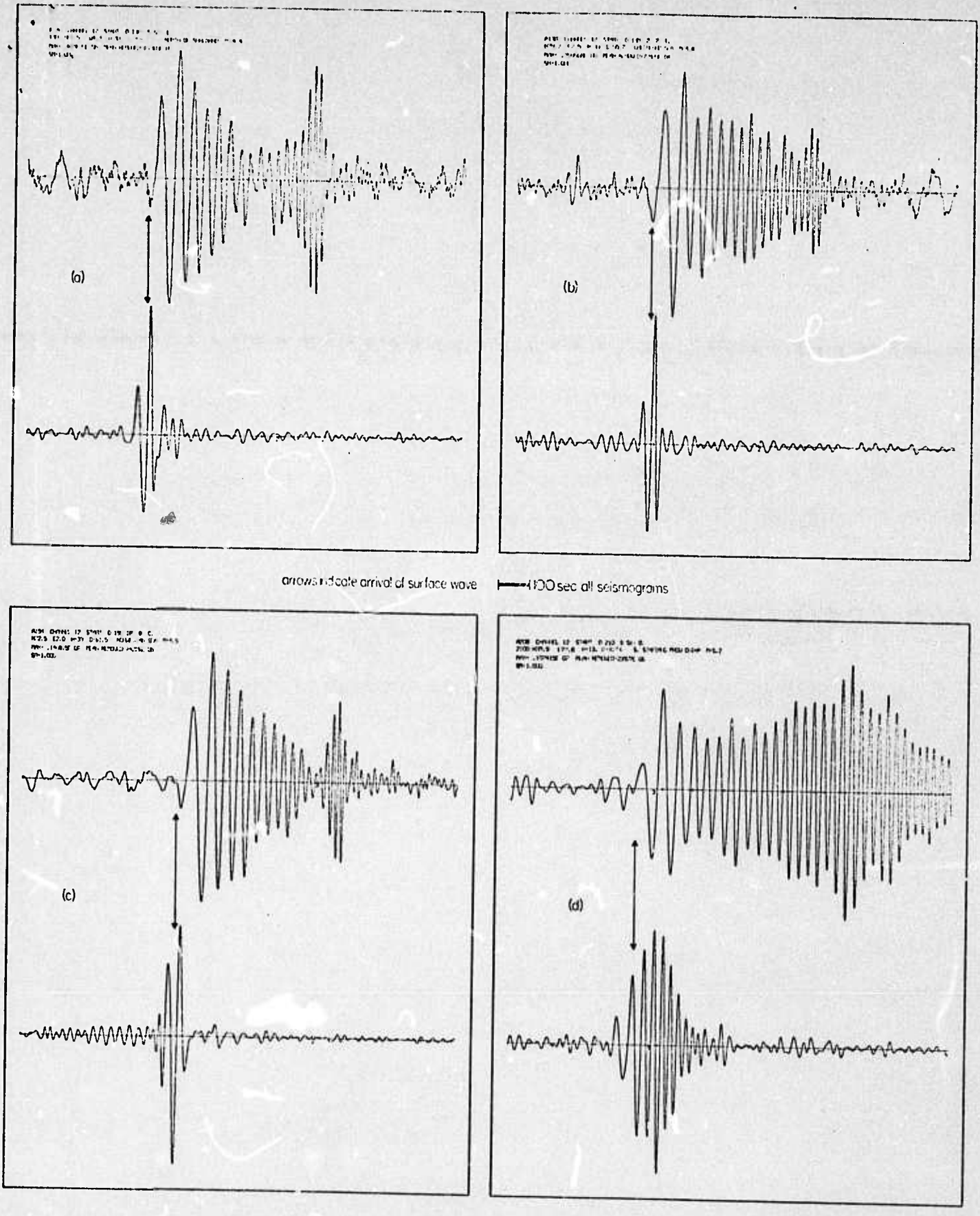

arrows indicate arrival of surface wave ⟵100 sec all seismograms

Figure 7

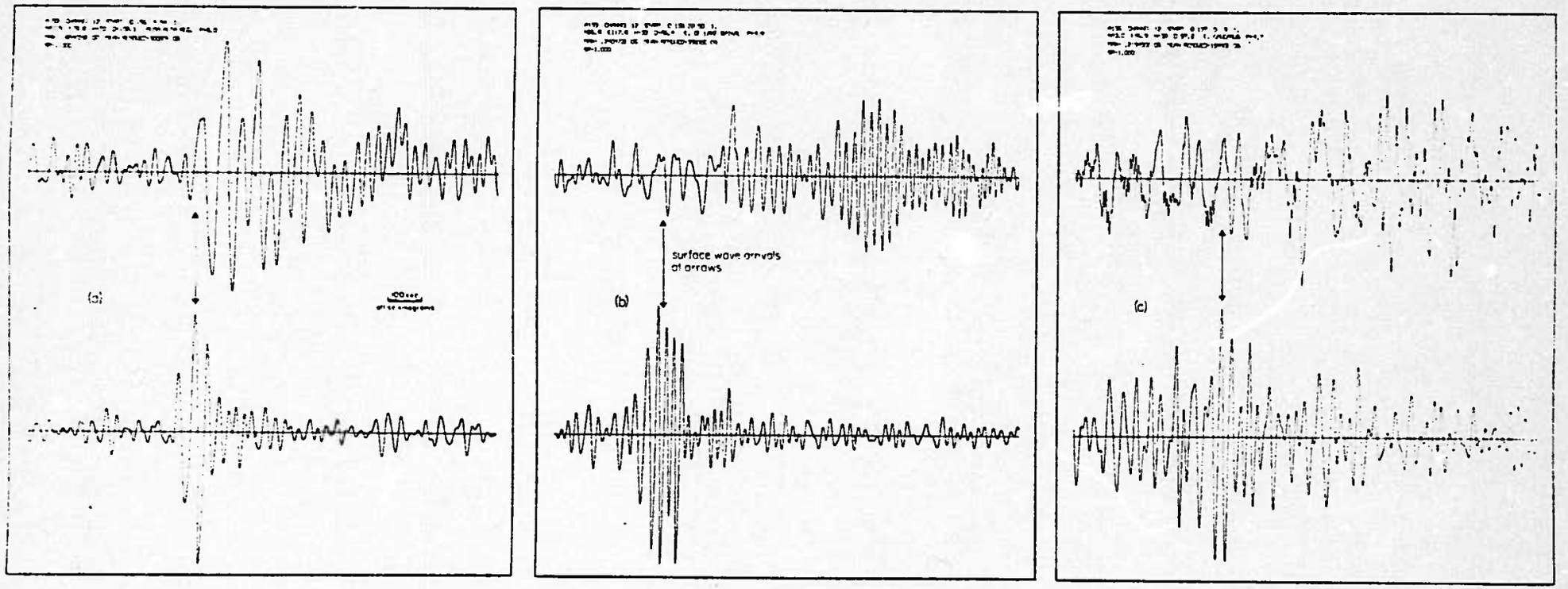

Figure 8

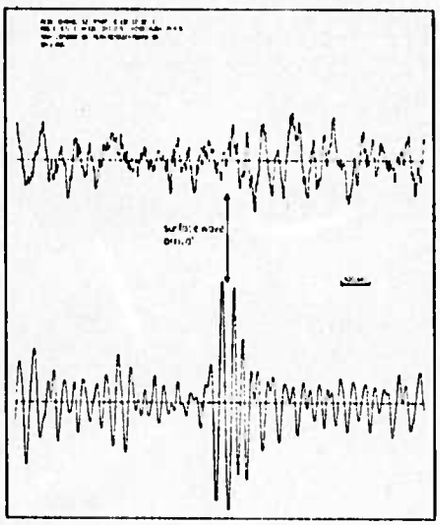

Figure 9

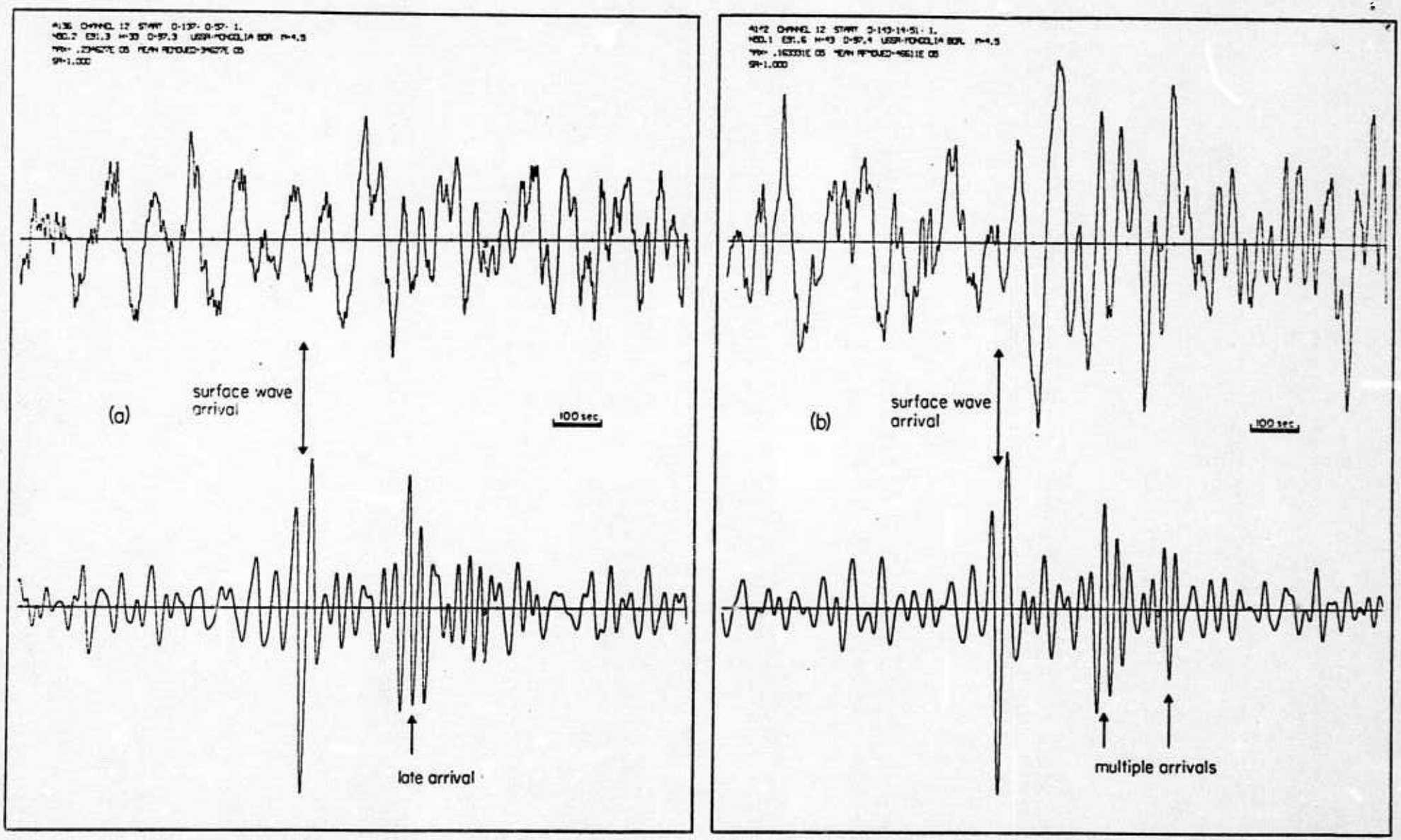
(a)
surface wave arrival
100 sec.
late arrival
(b)
surface wave arrival
100 sec.
multiple arrivals

Figure 10

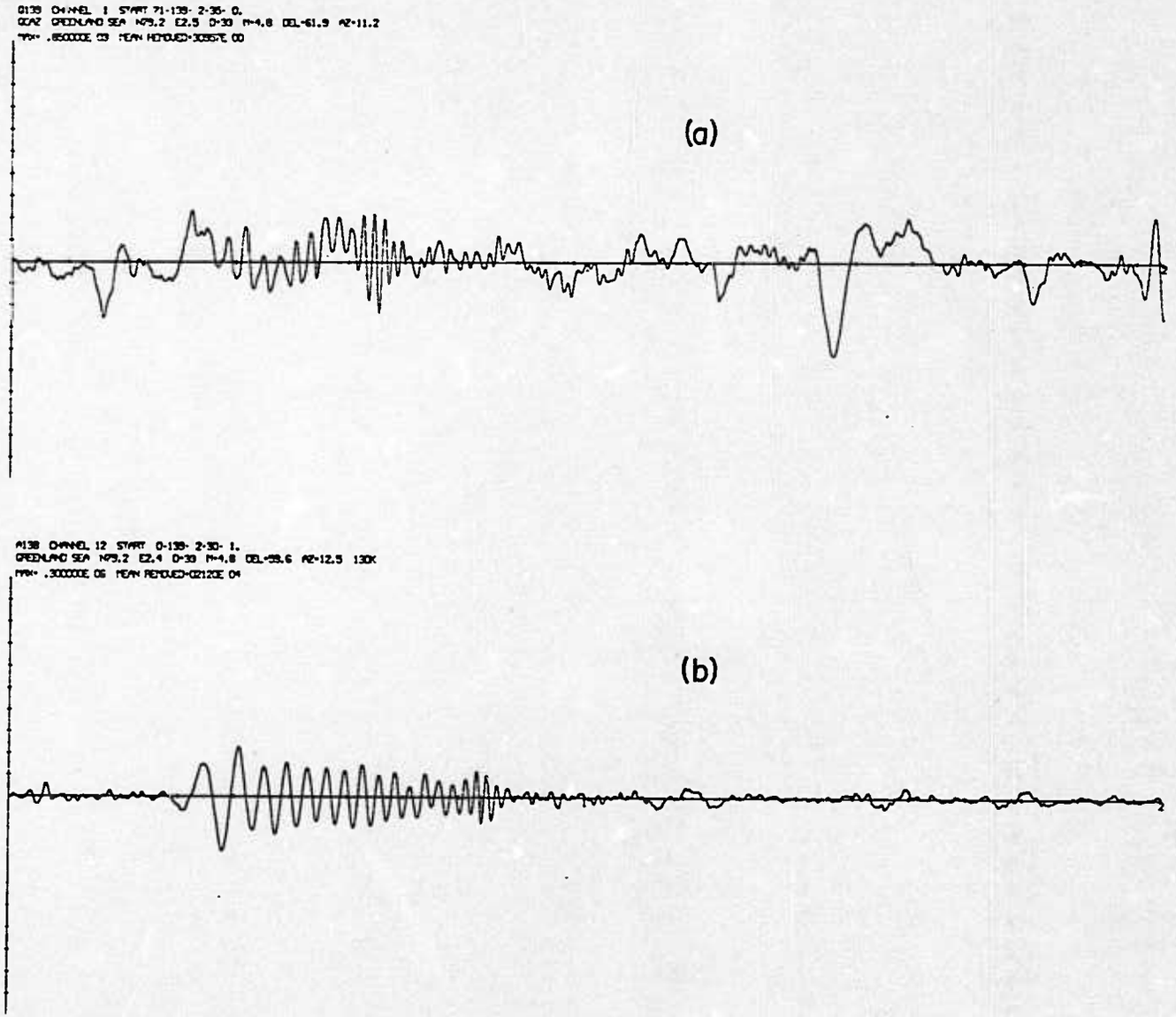
0139 CHANNEL 1 START 71-139- 2-35- 0.
GOAZ GREENLAND SEA N79.2 E2.5 D-39 M=4.8 DEL=61.9 AZ=11.2
MAX= .850000E 03 MEAN REMOVED=.3055?E 00
(a)
A138 CHANNEL 12 START 0-139- 2-30- 1.
GREENLAND SEA N79.2 E2.4 D-39 M=4.8 DEL=58.6 AZ=12.5 130K
MAX= .300000E 06 MEAN REMOVED=.02120E 04
(b)

Figure 11

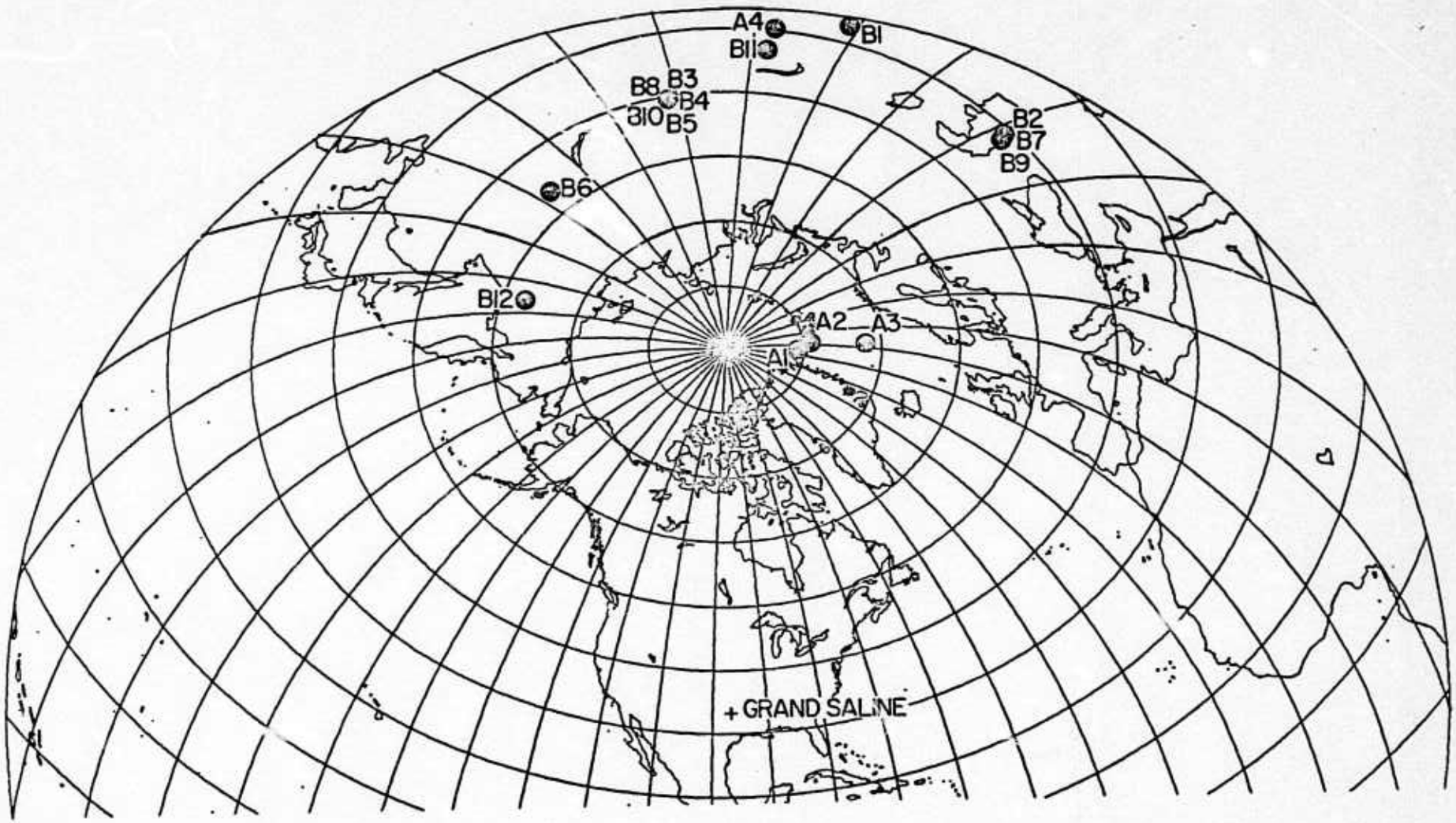

Figure 12

TABLE 1

Geographic Location	Origin Time[1] Year Day Time	Lat.[1] deg	Long.[1] deg	Depth[1] Km	m_b[1]	M_s[2]	Δ[3] deg	Azimuth[3] deg
A1. N. of Svalbard	70-130-055240·2	81.5N	4.7W	33	4.4	4.0	58.1	10.1
A2. Greenland Sea	70-139-020741.5	79.2N	2.5E	33	4.8	3.7	59.7	12.5
A3. Norwegian Sea	70-195-180637.8	72.5N	2.0E	33	4.9	3.9	61.5	20.0
A4. S. Sinkiang Prov.	70-210-055056.4	39.9N	77.8E	13	5.2	5.4	107.6	5.2

1. From NOAA PDE cards

2. Calculated from Gutenberg (1945) using calculated Δ

3. Calculated from coordinates of epicenter and of recording station:

   Grand Saline Texas 32° 39' 19" N)
   95° 42' 10" W)

(Same footnotes apply to table 3.)

TABLE 2

Group Velocity	Period
3.9250	75.5223
3.8750	69.2352
3.8250	60.8679
3.7750	51.8606
3.7250	45.6151
3.6750	41.9743
3.6250	39.5603
3.5750	37.4096
3.5250	35.5422
3.4750	34.0502
3.4250	32.0733
3.3750	30.5458
3.3250	29.3486
3.2750	27.7666
3.2250	26.1123
3.1750	24.6726
3.1250	23.4360
3.0750	21.3606
3.0250	19.2884
2.9750	18.6214

TABLE 3

	Geographic Location	Origin Time Year - Day - Time GMT	Lat[1] deg	Long[1] deg	Depth[1] km	M_b[1]	M_s[2]	Δ[3] deg	Azimuth[3] deg
B1.	Hindu-Kush	70-130-123233.3	36.1N	71.1E	121	4.7	?	110.5	11.4
B2.	E. Caucasus	70-135-061916.6	43.1N	47.3E	33	4.5	3.2	97.4	26.4
B3.	USSR-Mongolia Bd.	70-135-171315.1	50.2N	91.3E	33	5.9	5.7	97.3	355.5
B4.	USSR-Mongolia Bd.	70-135-185007.4	50.3N	91.2E	33	4.6	4.9	97.2	355.5
B5.	USSR-Mongolia Bd.	70-135-201216.9	50.2N	91.3E	33	5.0	4.3	97.3	355.5
B6.	E. Lake Baikal	70-135-205012.7	56.8N	117.8E	33	4.9	4.3	86.5	342.3
B7.	E. Caucasus	70-136-104323.0	42.9N	47.1E	33	4.4	3.3	97.4	26.6
B8.	USSR-Mongolia Bd.	70-137-005648.0	50.2N	91.3E	33	4.5	3.4	97.3	355.5
B9.	E. Caucasus	70-137-050217.7	43.0N	46.9E	33	4.7	3.4	97.3	26.7
B10.	USSR-Mongolia Bd.	70-143-145134.6	50.1N	91.6E	43	4.5	3.4	97.4	355.3
B11.	Alma-Alta Rgn.	70-156-045306.4	42.5N	78.8E	20	6.0	5.7	105.1	4.2
B12.	E. Siberia	70-156-103154.3	63.4N	146.2E	33	5.5	4.5	72.5	335.4

(For footnote see table 1)